Modern Mechanical Engineering, 2022, 12, 27-44
https://www.scirp.org/journal/mme
ISSN Online: 2164-0181
ISSN Print: 2164-0165

Finite Element Structural Analysis of Buried Pipelines

Casanova-del-Angel Francisco, Córdova-Castillo Alejandra

Escuela Superior de Ingeniería y Arquitectura, UP ALM, SEPI of the Instituto Politécnico Nacional, Mexico City, Mexico
Email: fcasanova49@prodigy.net.mx, arq.alex_cordova@gmail.com

How to cite this paper: Francisco, C.-del-A. and Alejandra, C.-C. (2022) Finite Element Structural Analysis of Buried Pipelines. *Modern Mechanical Engineering*, **12**, 27-44.
https://doi.org/10.4236/mme.2022.122002

Received: February 18, 2022
Accepted: May 7, 2022
Published: May 10, 2022

Abstract

This document uses previous results (which we call the first stage), for the development of a computer model based on finite elements under the FEAP programmer, to carry out a structural analysis of a pipeline. For this purpose, we used environmental variables that we believe influence the failure of buried pipelines such as the internal pressure of fluid, the type of support used, the temperature at which the pipelines work, the type of soil and the stiffness of the soil acting on it. Once the model was finalized, analyses were made with each of the variables separately and combined to observe the behavior of the pipeline, finding the most unfavorable case that indicates the main causes that led to its failure.

Keywords

Duct, Finite Element, Buried Pipeline, Material Creep, Thermal Conditions, Soil Springs

1. Introduction

This document contains the results of the second stage of research on the structural behavior of buried pipelines designed to transport fuels, to determine and study the causes that lead to the expansion of cracks in them, using the simulation of a finite element model (first stage), using the results obtained in metallographic, chemical and mechanical tests. In this first stage, the research included studies to determine the material composition, resistance and the conditions in which the pipeline was physically found when it was taken out of operation, which are not described here. After the laboratory tests were carried out, the physical and chemical characteristics were analyzed and compared with the API 5L, ASCE, NRF-001-PEMEX and NRF-030-PEMEX standards, which finally led to a specific characterization of the conditions of the sample. According to the standards, the grade of the pipeline was between X65 and X70 [1].

Before presenting the results, it is necessary to ask why this study is important. The oil and gas industry has led to large-scale construction of high-capacity infrastructure that allows fuels to be transported over long distances at a very low cost. The main pipeline builders are the oil companies. They have pipelines for the collection of crude oil and gas from extraction wells, for transportation to refineries, petrochemical and gas processing complexes, as well as for the distribution of final products to storage terminals and end consumers. Other pipeline construction companies are electricity generating companies, in order to supply gas to their power plants. There are also natural gas pipelines that cross entire cities, as well as those built by and for the service of large industrial users. Unlike other hazardous industrial facilities, pipelines are not within an industrial complex with safety features; instead, they are deployed across land owned by third parties, between cities and highways, or through agricultural land, rivers, oceans and natural sites, including private properties, agrarian communal lands, protected natural areas and indigenous territories. Therefore, in the event of a hydrocarbon leak, the risk of spills, contamination and explosions is extremely high, ranging from 20 meters for small diameter pipelines to more than 300 meters for large or high-pressure pipelines. Pipelines are almost always buried; however, their construction, supervision and maintenance require extensive rights of way and a terrain clear of vegetation.

Concerning its regulatory framework, pipeline transport can be extremely complex, and to understand it, it can be categorized by: company, type of hydrocarbon, diameter, the function performed, the current state of operation, among others. The analysis by categories provides clarity on various aspects. It is easiest to distinguish between collection pipelines and transport and distribution pipelines. But to put historical spills in context, it is necessary to know that: oil spills are expressed in tons of crude oil where 1 ton is equal to 1000 kg, approximately 7.33 barrels and that since the 1940s (20th century) 7647393.14 tons of oil have been registered. Both at sea (ships and deep-water wells) and on land (pipeline fracture due to poor construction, corrosion, fractures due to external causes and poor maintenance, et cetera).

However, ducts in particular have an accumulated interior dirt problem. They have to be cleaned and special devices are used for this purpose. The main ones are called pigs. What is a pig in the oil industry? Pigs are devices that are inserted and travel the length of a pipeline, driven by the flow of the pipeline. There are two categories: Polly Pigs and Cleaning Devils which are basic cleaning elements. Their main function is to clean and remove sediment within the pipeline. The second category refers to intelligent or instrumented pigs which provide information on the status of the line, as well as the extent and location of any problems or abnormalities in the line. The history of pigs is interesting and probably has a large degree of fiction, but it is always good to hear what the pig-running world recognizes as their origin and peculiar name. The first devil running operation is said to have taken place around 1870, a few years after Colonel Drake discovered oil in Titusville, Pennsylvania.

In order to determine the problem that we are studying, it is also necessary to be aware of the number of pipelines that exist in the world (Table 1).

Table 1. Existing pipelines as of 2015 [2].

Location	Diameter	Length	Start of operation
Libya-Italy	80 cm	540 km	7 October 2004
Tanzania-Zambia-Mafuta	20 - 30 cm	1710 km	1965
Chad-Cameroon	75 cm	1070 km	2003
Algeria-Morocco-Spain-Portugal	120 - 70 cm and 55 cm	1620 km	1 November 1996 the Algeria-Morocco section. 9 December 1996 for the Spanish section and 27 February 1997 for the Portuguese section.
Sudan-South Sudan	70 cm	1600 km	18 June 1999
Russia-Latvia-Lithuania-Belarus-Belarus-Ukraine-Slovakia-Czech Republic-Poland-Germany	42.5 cm	8900 km	15 October 1964
China (Xinjiang-Shanghai)	85 cm	8704 km	1 October 2004
Azerbaijan-Georgia-Turkey	85 - 105 cm	1768 km	10 May 2005
Russia-Belarus-Belarus-Poland-Germany	140 cm	2000 km	1997
Turkmenistan-Uzbekistan-Kazakhstan-China	105 cm	1833 km	12 December 2009
Croatia-Serbia-Hungary-Slovenia-Slovenia-Bosnia and Herzegovina	50 cm	525 km	1989
Netherlands-United Kingdom	90 cm	235 km	1 December 2006
Norway-United Kingdom	105 - 110 cm	1166 km	16 October 2006
France-Switzerland-Germany	85 cm	769 km	1962-1963
Italia-Austria-Alemania	85 cm	753 km	1967
Australia	65 cm	502 km	February 2006
Australia	65 cm	797 km	January 2003
Longford (Australia)-Bridge water (Tasmania)	62.5 - 75 cm and 120 cm	740 km	August 2002
Australia	35 - 40 cm	1378 km	September 1994
Australia	65 cm	1789 km	1985
Bolivia-Brasil	90 - 80 cm	3150 km	June 1999
USA	90 - 105 cm	2702 km	January 2015
Argentina	60 - 75 cm	3756 km	1978
Canada (Alberta-Quebec)	120 cm	3227 km	10 October 1958
Canada and USA	75 cm	3456 km	January 2014
Mexico	75 cm	68843.15 km	Since 1890
Total number of kilometres of pipelines		**123532.15 km**	

Let's move on to the technical-scientific part of our study. In engineering, continuous structures are common (pipelines), and for their analysis, it is necessary to use a method that takes into account the continuity of the material and its structure. The finite element method can model a continuous medium using a set of defined and differentiated elements, which are connected by a series of points resulting in a mesh. The main objective of the method is to analyze the behavior of a continuous medium that is discretized into simple geometric forms, enriching the solution of numerical problems in engineering, since in recent years it has had multiple applications thanks to the fact that its development has gone hand in hand with the technological advance of computers. Some of the representative works on the subject, we can mention the following.

Within the theme of this study should be mentioned a publication that aims to analyze the behavior of the underground part of steel pipelines under the effect of loads caused by internal pressure and temperature variation due to transportation of hydrocarbon products. The pipeline under study was buried in a sandy soil, four parameters being studied: the length of the buried part of the pipe, the properties of the soil, the depth of the soil cover and the final condition of the buried part of the pipe. It is found that increasing the length of the part of the pipeline or increasing values of the normal and tangential modulus of subgrade reactions for the surrounding soil causes decreasing in the values of longitudinal displacement, stress, and strain. Soil cover depth over buried pipeline has no effect on the longitudinal displacement, but the stresses and strain increased when the soil cover depth increases. From studying the effect of boundary conditions of the two ends of steel buried pipeline, it is found that longitudinal maximum displacement did not affect, but the longitudinal stresses and strains increase with small rate values [3].

There is a document that states the impossibility of accurately estimating the seismic behavior of a buried pipe due to the uncertainty of both the characteristics of the soil and the seismic load. So, it was necessary to evaluate both the static and pipe behavior to determine the probability of buried pipe behavior. It examines the typical behavior of the pipe caused by static and seismic load according to the types of soil and a degree of saturation in the soil considered, all with the finite element method. It is claimed to have carried out assessments on the behavior of a buried pipe according to soil types, the degree of saturation in the soil and the types of loads [4].

The work starts from theoretical concepts of failure due to plastic instability in thin-walled pressure vessels and are confronted with the results obtained from an experimental laboratory model and based on the mechanics of the fracture the failure condition is presented by having a crack-type defect. The laboratory model was made of aluminum, without specifying whether this is structural aluminum and of what type, and show that, with a low fluctuating pressure a crack can grow to a critical fault size after a certain number of pressure cycles. It is concluded that by pressure fluctuation and/or cracking by corrosion under stress a stable crack growth can be presented until obtaining a critical fault size with a pressure lower than the failure pressure due to plastic instability or less than the creep failure pressure [5].

Oil and gas pipelines are usually buried in ground to provide protection and support. Buried pipeline may experience significant loading as a result of relative displacements of ground along their length in the case of a buried pipeline, forces are statically indeterminate because the characteristic of soil is not uniform (Watkins and Anderson, 2000). The present paper is to analyze the pipeline buried in soil using CAESAR-II software. Main aim of piping stress analysis is to provide adequate flexibility for absorbing thermal expansion, code compliance for stresses and displacement incurred in buried piping system. The design is safe when all these are in allowable range as per code. In this study, a pipeline buried in soil is considered for analysis as per power piping ASME B31.1 code and the results thus obtained are analyzed. This paper also examines the typical pipeline behavior caused by static load in accordance with soil types and a degree of saturation in considered soil. The finite element method (FEM) is selected as the examination method for the underground piping system [6].

Finite-element analysis applied to flexible pipe systems requires capabilities not included in conventional finite-element analysis computer programs. Because of the flexibility of the fiberglass-reinforced plastic pipe and other pipes of similar flexibility, the finite-element analysis may need to accommodate large deflections. In addition, the sensitivity of the pipe and the soil properties to compaction loading should be considered. In this study the stress history of the soil elements was monitored at each loading increment to determine whether each element was to be analyzed by using primary loading nonlinear elastic parameters or unloading and reloading stress-dependent elastic parameters. The development of the additional features of the finite-element computer program allowed for applications to buried flexible pipe when subjected to various installation conditions, backfill material types, surcharge loadings, and internal pressurization. Results of the finite-element analysis applications were compared with measured pipe responses from similar soil-box installation conditions. The features of the finite-element analysis computer program and results for a silty sand backfill material under several installation conditions are described. The results are compared with the measured response of the pipe from soil-box tests [7].

Below, we describe the characteristics of the conditions and actions to which the pipeline under analysis was subjected, as well as the characteristics of the finite element model.

2. Description of the Model

The data used for the development of the model geometry, mesh distribution, constraints, acting forces, type of material and its properties, type of analysis and visualization of graphs and images is registered. The first step for the execution of the analysis is to elaborate a starting file; **Table 2**. The geometric workspace is

Table 2. Data required for the construction of the grid.

FEAP: Project. PIPE SUBJECTED TO LOAD Input Data Filename: Itub.txt	
Number of nodal points	2296
Number of elements	960
Spatial dimension of Mesh	3
Degrees of freedom/node (Maximum)	3
Equations/Element (Maximum)	0
Number elements nodes (Maximum)	8
Number of material sets	1
Number Parameters/Set (Program)	250
Number Parameters/Set (Users)	50

developed in three dimensions, contains three degrees of freedom per node and eight integration points for each element of the mesh.

Then the geometry created by a set of control points called super nodes is defined to establish the coordinates of the nodes in the Cartesian plane and form a polar (or cylindrical) surface. Only an arc showing a quarter of the model duct was created by a block of nodes and elements that are at the same time divided to create the mesh in all three dimensions, using six divisions around the circumference, one across (in thickness) and 40 longitudinally. Finally, the above was converted into a region, **Figure 1**.

The above region has been repeated three times and joined together to create a single region that draws the full circumference of the model. This is how the geometry of 2296 nodes with a mesh of 960 elements measuring 30 × 1.18 × 0.7 cm, or 24.78 cm^3, has been schematized, **Figure 2**.

Finally, the derived geometry is 1200 cm long, 9.0 cm (3 1/2") external diameter and 0.7 cm thick, **Figure 3**.

2.1. Working Conditions of the Model

The actions to be considered for the calculation of buried pipelines are: their own weight and that of the material they carry, effects caused by the type of terrain, the type of pipeline support, the amount of traffic where it is buried, the internal pressure caused by the fluid it transports, the temperature and the seismic conditions of the place where the pipeline is located, among others. The model is not intended to design the entire pipeline, however, for a better analysis, four of the above-mentioned conditions that participated in the failure of the pipeline have been taken into account, such as internal pressure, soil stiffness, temperature and its weight [8] [9] [10].

2.2. Requirements

The stresses, described below, are the internal pressure, the self-weight of the pipeline and the temperature. The acting internal pressure was the first starting

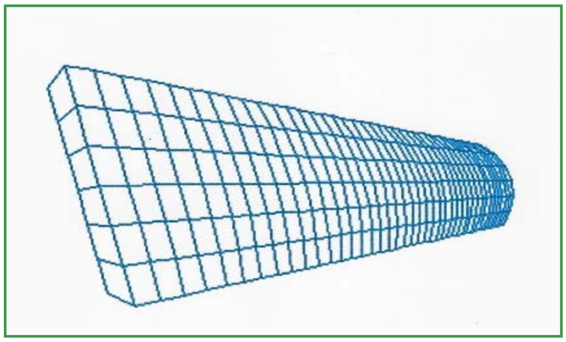

Figure 1. Region 1 of the grid.

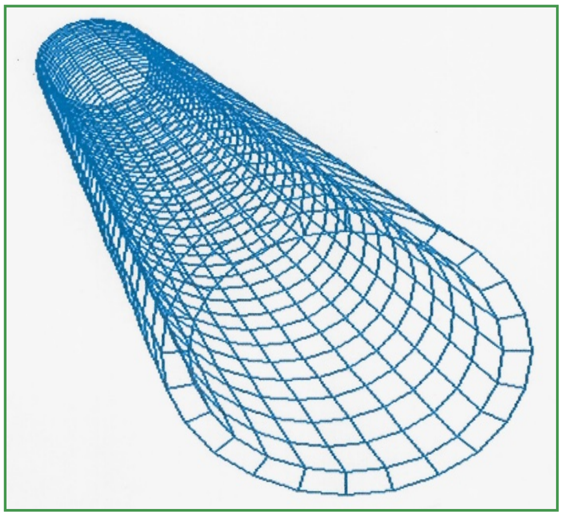

Figure 2. Final mesh of the model.

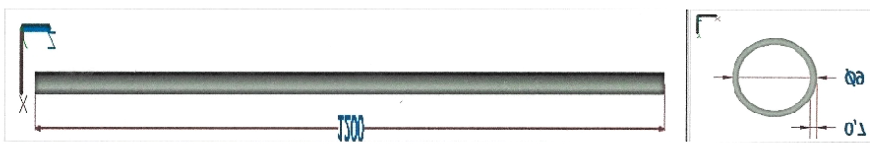

Figure 3. Longitudinal and cross-sectional view of the duct model.

point.

To obtain some of the data on the working operation stresses of the pipeline under study, the API 5L/2004 6, ASME B31.8/2007 [11] and NRF-030-PEMEX-2009 [12] standards were used. Considering that these standards used for the requirements of high-risk waste pipelines change every five years and that the pipeline was physically degraded due to the withdrawal time of its exposure to the environment, the results of the calculated stresses may present some variations to those currently used.

According to API standard 5L, 6, the pressure is calculated using Equation (1):

$$P = \frac{2St}{D} \tag{1}$$

where P is the hydrostatic pressure in psi (lb/in^2), S is the yield stress in psi, which is equal to the percentage of the minimum yield stress specified in **Table 3**, t is the specific wall thickness (expressed in inches) and D is the specific outside diameter (in inches), S is the specific wall thickness (in inches) and D is the specific outside diameter (in inches).

With the laboratory tests, yield stress of 110018 psi (7735.37 kg/cm^2) was obtained, which, when comparing the data with the specifications found in the API 5L standards, the grade of the pipe with similar characteristics is X70.

According to the above, the analytical solution is given in (2):

$$P = \frac{2(66010.8\text{ psi})(0.2755\text{ in})}{3.5\text{ in}} = 10391.98\text{ psi} \quad (2)$$

therefore, the result of the internal pressure that the duct could withstand is 10391.98 psi. (730.66 kg/cm^2).

For the calibration of the pressure within the analysis model, it was necessary to transform the pressure using elementary forces under the given procedure on stress in thin-walled cylinders.

$$F = (730.66\text{ kg/cm}^2)(7.6\text{ cm})(30\text{ cm}) = 166440.0\text{ kg} \quad (3)$$

This resultant force only affects half the circumference of the duct and the first section of the mesh, which is equal to 30 cm. The force obtained in (3) was divided by 24, which represents the number of nodes in that section, resulting in a force of 6935 kg per node, Equation (4).

$$F = \frac{166440\text{ kg}}{24\text{ nodos}} = 6935\text{ kg} \quad (4)$$

To determine the forces within the analysis model it was necessary to employ a process to assign the duct driving forces or loads (internal pressure) to each of the nodes around the circumference of the pipe, **Figure 4**.

Table 3. Specified minimum percentage yield stress to determine S, [13].

Grade	Specific outside diameter D mm (in)	Percentage of the specified minimum yield stress to determine S	
		Standard pressure test	Alternative pressure test
A25	141.3 (5.563)	60	-
A	≥60.3 (2.375)	60	75
B	≥60.3 (2.375)	60	75
X42 to X80	≤141.3 (5.563)	60	75
	>141.3 (5.563) a ≤219.1 (8.625)	75	75
	>219.1 (8.625) a <508 (20.00)	85	85
	≥508 (20.00)	90	90

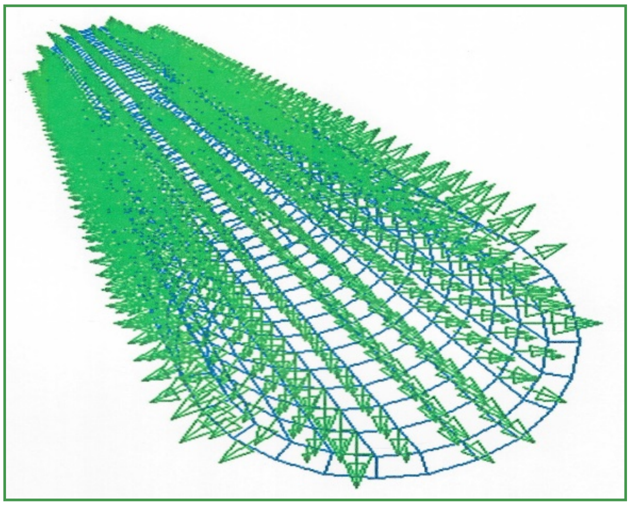

Figure 4. Internal pressure view of the model.

The self-weight of the duct and the thermal conditions were determined as part of the analysis process. To include the dead weight, it was necessary to calculate the mass and specific gravity (ρ) of the material, in this case steel. The weight of the steel is 7.85 T/m^3. The mass has been calculated by multiplying the specific weight of the steel by the volume ($V = 0.022\ m^3$) of the pipe and all this is divided by the gravity ($g = 9.81\ m/s^2$). The analytical solution is given in (5):

$$m = \frac{\rho V}{g} = \frac{\left(7.85\ \text{T}/\text{m}^3\right)\left(0.022\ \text{m}^3\right)}{9.81\ \text{m}/\text{s}^2} = 0.017\ \text{Tonf} \tag{5}$$

and the result of the mass in kg units is 0.176 kgf.

The thermal conditions used in the analysis were an ambient temperature of 20˚C (68˚F) because this is a standard temperature as it was only intended to observe its influence on the failure of the pipeline.

2.3. Boundary Conditions

For a more realistic analysis, where the behavior of the complete pipeline could be appreciated, it was considered that it would be 1200 cm long. The boundary conditions applied in the model were defined so that each end of the pipeline was constrained, as well as an adequate simulation that the pipeline was buried. To begin with, the support conditions were assigned, located at coordinates 0.0 and 1200.0 of the 3-z reference axis to create the rigid supports in the three directions of each node around the circumference, as can be seen in **Figure 5**.

The second boundary condition used for the analysis was the soil in which the pipe was buried. The weight of the soil on the pipe is represented by discrete non-linear springs, which were exerted in the analysis using a command that allowed the springs to be located along the entire length of the pipe. Four lines of springs were placed along the length of the model along the z-axis: two along the x-axis to represent the lateral stiffnesses and two along the y-axis for the vertical stiffnesses, as shown in **Figure 6**.

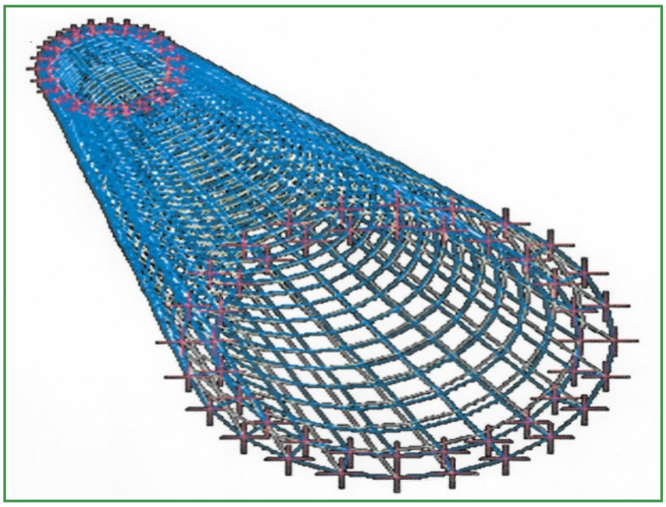

Figure 5. Constraints in the model.

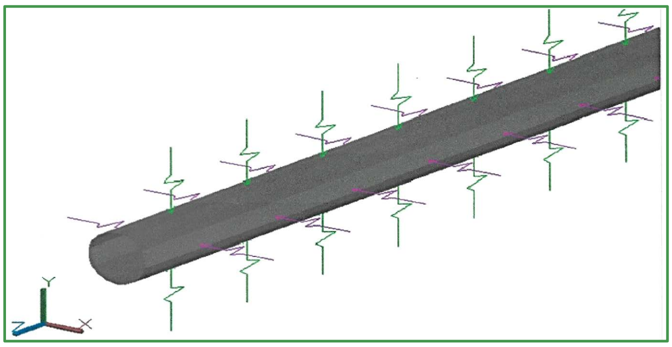

Figure 6. Location of the springs in the model.

The maximum soil spring forces and associated relative displacements required to develop these forces were calculated using equations based on the ASCE 2001 standard [14].

Before assigning the data required in the calculation of the springs, the type of soil to which the pipeline was subjected should be described.

One characteristic that makes each soil type different is cohesion. Because of cohesion, soils are classified as cohesive and non-cohesive. Cohesive soils are those that possess the property of intermolecular attraction, such as clays. Non-cohesive soils are soils consisting of rock particles without any foundation, such as sand and gravel [15].

As the soil in which the pipeline was buried was clay, the variables required in the formulas were assigned: soil cohesion (c) of 10 T/m^2, a specific gravity (γ) of 1.75 T/m^2, the adhesion factor (α) of 0.4, the angle of friction of cohesive soils equal to 0, the factors $Nc = 5.14$, $Nq = 1.0$ and $N\gamma = 0.0$. The other data external to the soil were the duct diameter (D) of 9.0 cm and the depth from the Centre of the duct to the ground surface (H), equal to 40.5 cm.

According to the above data, the results obtained for the axial spring rigidity (6), for the lateral spring stiffness (7) and the vertical spring stiffness (8) are:

$$T_u = 1.13 \text{ T/m} \tag{6}$$

$$N_{ch} = 6.7215 \leq 9$$

$$P_u = 6.05 \text{ T/m} \tag{7}$$

$$Q_d = 4.69 \text{ T/m} \tag{8}$$

The above values completed the first phase of the pipeline analysis.

2.4. Model Solution

The material was assigned as a solid type element with the properties of steel for analysis: plane stress and isotropic elastic material type with a modulus of elasticity of 2,030,000 kg/cm^2 and a Poisson's ratio of 0.3.

A load cycle from 0 to 100% of the load value was defined. To check that these values were correct, a previous analysis was made where only the pressure load was considered and as a result the creep value was similar to the one obtained in the laboratory tests, 1. During the model analysis, the behavior of the duct due to the boundary conditions, the support conditions and the material properties used in the model were observed, illustrating with colors the maximum (red) and minimum (blue) stresses. In this way, the most stressed nodes were located and their graphs and images were obtained. After carrying out the analysis process several times, the number of the node where the greatest stresses were concentrated was calculated, thus obtaining the value at each time step with the results of the stresses and displacements at that node according to the loading process.

3. Results of the Pipeline Model Analysis

Next, the analysis of the pipeline with the different boundary and load conditions described above is presented. For the behavior of the pipe, a loading cycle of five-time steps was presented, in which it started with a zero load and ended with the maximum support load of the pipe according to the data obtained from the internal pressure.

The development of this analysis has been divided into four analysis processes: with pressure only; pressure and springs; pressure and thermal; and the final one is the combination of the above (pressure, springs and thermal). The parameters that did not move in any of the cases were the self-weight of the duct and the support conditions.

3.1. Duct Analysis Using Internal Pressure

To observe the behavior of the duct, only the load generated by the internal pressure was used. As a result, the following images and graphs were obtained.

Figure 7 shows how the duct is radially stressed, *i.e.* under pressure it expands in its radial directions. At an internal pressure the stress has a value of 7200 kg/cm^2.

The largest displacements occur at the center of the duct because the buckling on both sides prevents movement. Figure 7 shows how a double embedded beam buckles in the center of the duct.

Figure 8 shows the behavior of the duct that was generated by pressure alone.

Figure 9 shows the graph that indicates that the duct has a linear behavior until it reaches the creep of the material, which we obtained in the laboratory tests Ibid. This means in effect, that the model developed gives values close to the real ones, which means that it is well calibrated.

3.2. Duct Analysis Using Internal Pressure and Soil Springs

Internal pressure and soil springs were used in this analysis. The results obtained were:

Visually, the behavior of the duct shows different values, like in the case of the previous analysis as shown in Figure 10. Since the forces act in the opposite

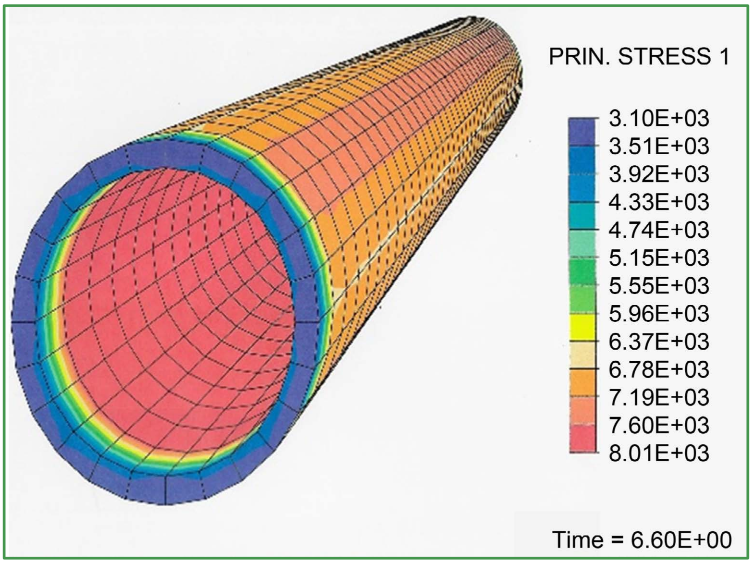

Figure 7. Principal stresses in direction 1 due to internal pressure.

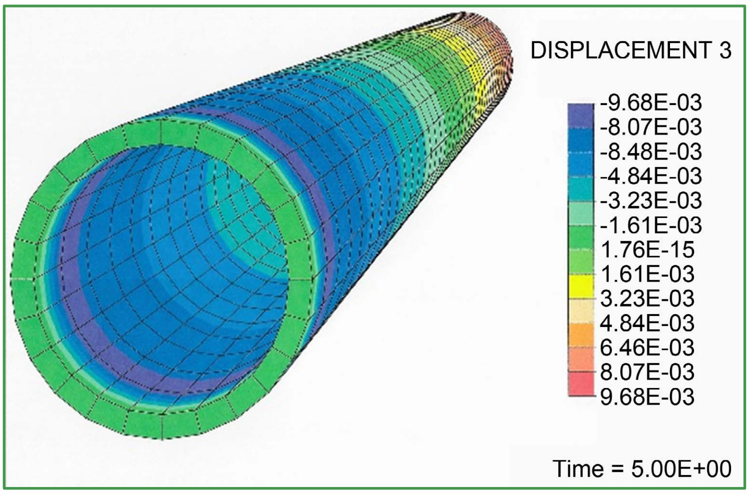

Figure 8. Displacements in direction 3 due to internal pressure.

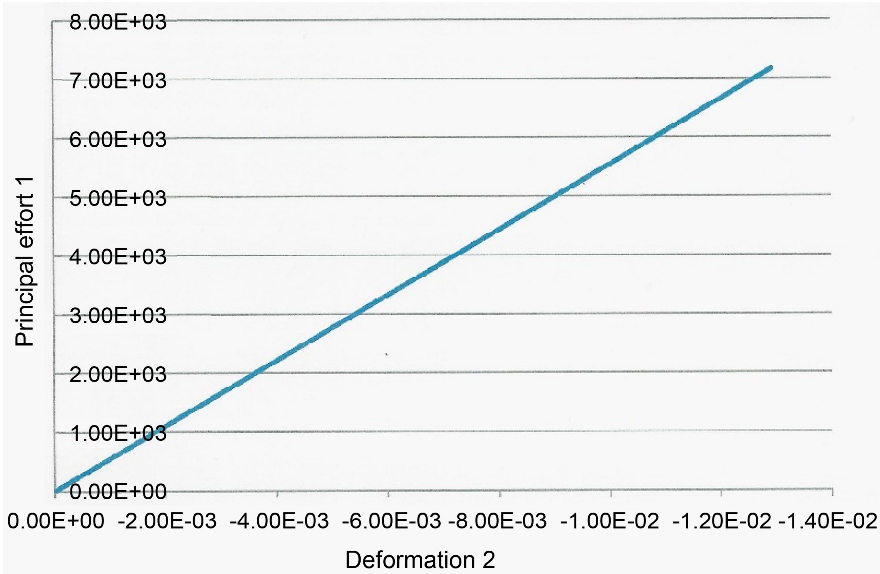

Figure 9. Principal stress-strain graph generated by internal pressure.

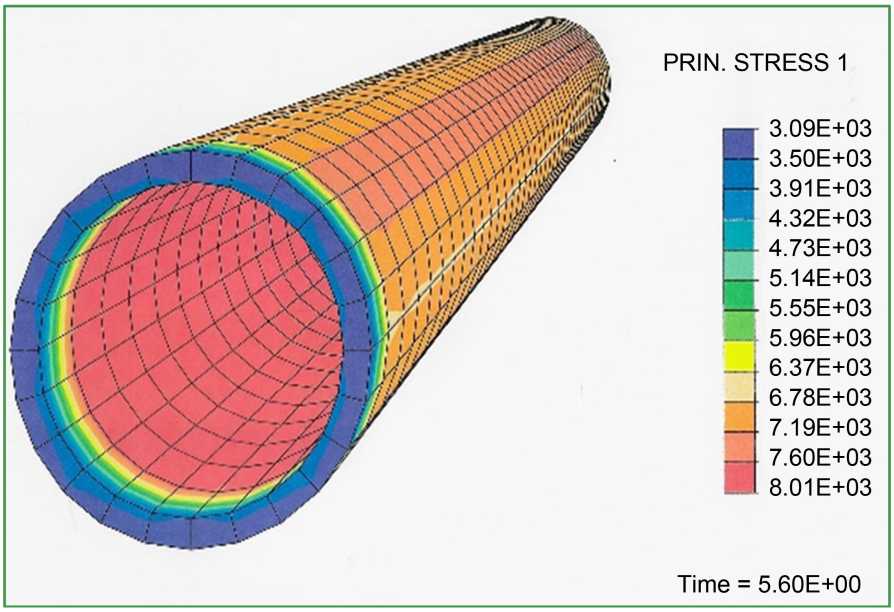

Figure 10. Principal stresses in the direction 1, obtained from the combination of internal pressure and soil springs.

direction, *i.e.*, the pressure tries to expand the element and the springs act towards the inside of the element, preventing it from expanding, both conditions cause the stresses to concentrate at the center of the thickness, but the internal pressure continues to have the greatest influence on the stresses.

The value of the displacements is higher than the previous ones, which is probably because it is as if a vertical load has been added due to the spring acting on the top of the tube, **Figure 11**. The behavior of the graph is still linear, **Figure 12**. The higher the stress, the greater the deformation of the duct, although these large-scale deformations are close to zero.

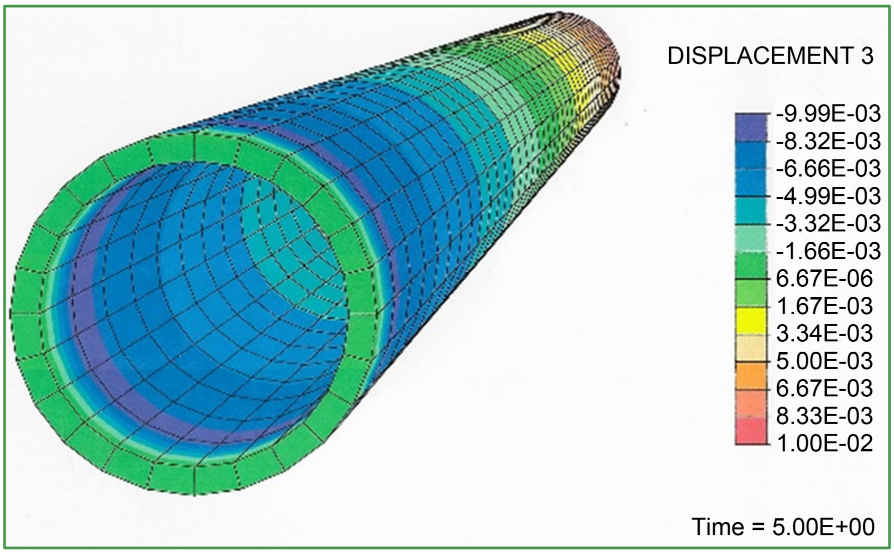

Figure 11. Displacements in direction 3 obtained from the combination of the pressure internal and floor springs.

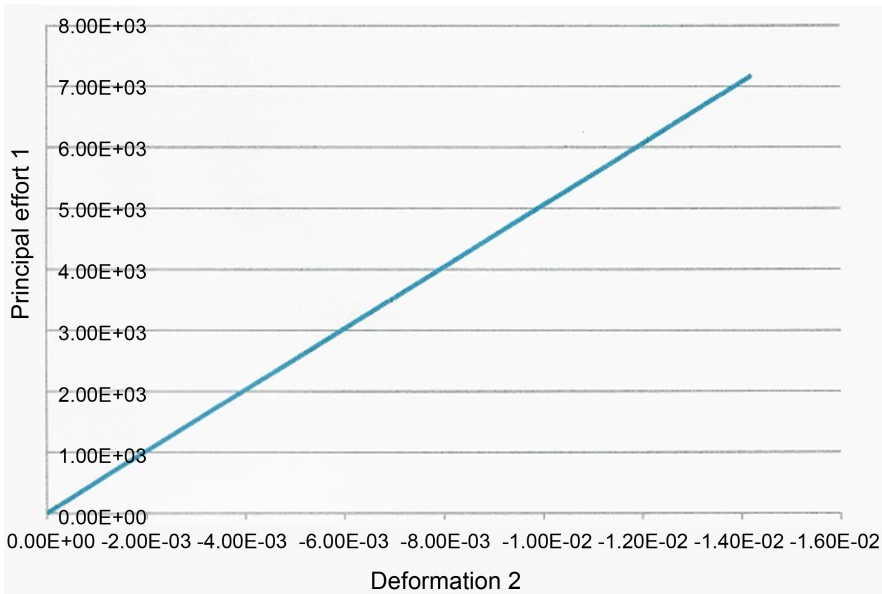

Figure 12. Principal stresses in direction 1 obtained by the combination of internal pressure and thermal.

3.3. Duct Analysis Using Internal Pressure and Thermal Condition

Another type of analysis was to use internal pressure and thermal conditions. The results obtained were:

It has the same stress process, but in this model, a temperature was implemented and therefore its behavior is different, Figure 12. The pressure transmits energy outwards from the element and together with the temperature causes the stress on the element surface to increase. The value of the highest stress increases to 7500 kg/cm^2.

This analysis of the displacements in direction 3, obtained from the combination of the internal pressure and thermal condition, is similar to the results obtained by applying only the internal pressure, Figure 13.

In combination with the thermal conditions, the duct starts to show a non-linear behavior, Figure 14. A body with thermal elements generates energy with the strength that acts upon it, therefore, based on a temperature value and knowing that the material is manageable at certain temperatures, it can show higher deformations.

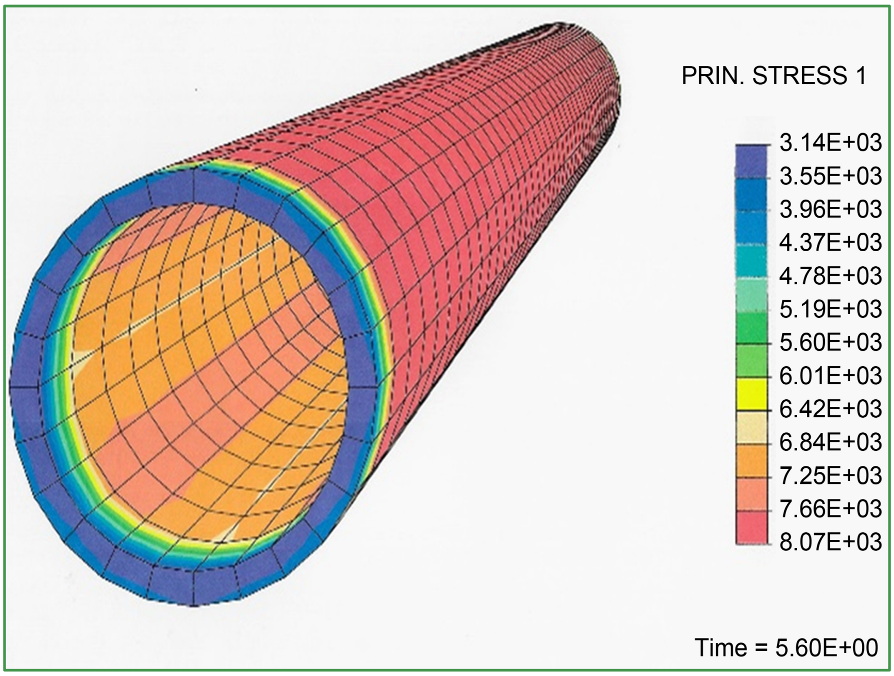

Figure 13. Displacements in direction 1 obtained from the combination of internal pressure and thermal condition.

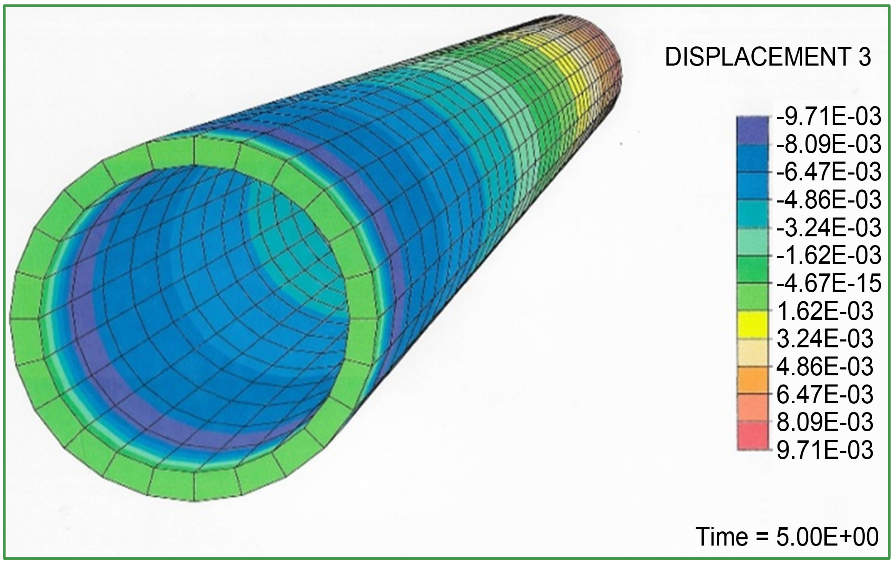

Figure 14. Principal stress—strain graph generated by the combination of internal pressure and thermal condition.

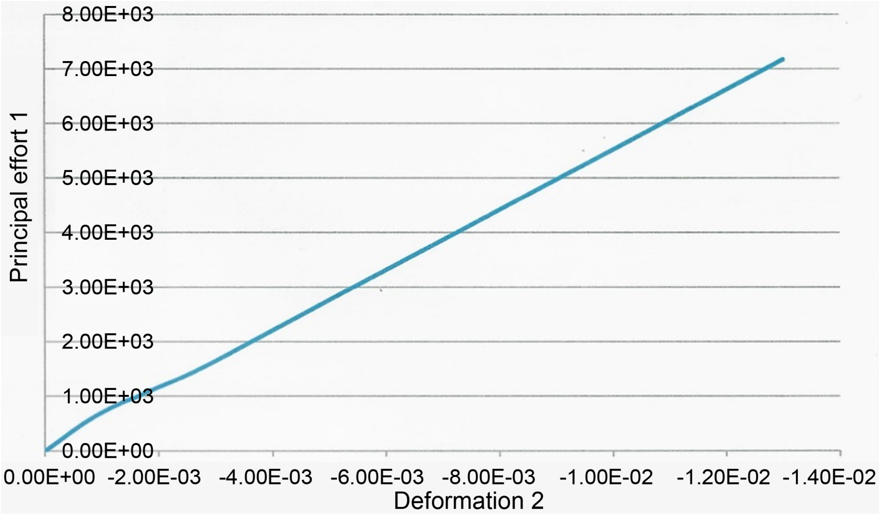

Figure 15. Principal stresses in direction 1 obtained from the combination of internal pressure, soil springs and thermal condition.

3.4. Duct Analysis Using Internal Pressure, Soil Springs and Thermal Condition

Finally, only the load generated by the internal pressure was used. As a result, the following images and graphs were obtained.

The pressure together with the temperature at which the element works and the springs that simulate the soil, cause the duct to reach its highest stress on the outside. This is due to the friction generated by the soil when the duct starts to expand at a certain temperature, Figure 15.

In another part of the study, the displacements according to the three working conditions to which the duct was subjected during the analysis process were observed. In terms of values, a balance was obtained from the three previous processes, but its value was closer to that of the process containing the springs. Finally, the combination of all the working conditions to which it was subjected, makes its behavior non-linear, therefore, the stresses become constant at some point before reaching the fracture. In this case, the behavior is varied from the beginning of the analysis process, *i.e.*, from the start, non-linear behavior is observed.

4. Conclusions

Linear-elastic analysis is commonly used in buried pipelines with high pressures, and generally, the elastic limits are exceeded. In addition, there is the pressure generated by the soil and the temperature at which the pipelines are working. A structured mesh represents a better analysis, ensuring better stress distribution and more realistic results.

Since the steel had a high carbon content, it contained many pearlite colonies which, in turn, degraded over time and caused the elastic range to be exceeded as a result of the stresses and boundary conditions that affected the pipeline. In its design, it is considered important that the pressure exerted by the fluid on it does not exceed the creep limit, otherwise a change of section must be made.

The results obtained in the analysis indicate that the variables together led to the failure of the duct. The carbon flakes separated and, upon reaching the grain boundary, caused the steel to lose its mechanical properties.

Finally, the temperature to which the duct was subjected had the greatest influence on the material exceeding its yield strength. This may be due to the fact that the steels are cast in order to be moulded and, therefore, the heat causes the material to degrade as the internal and external pressure of the duct influences it.

5. Future Research

We think it is interesting to study the effect of the trench surrounding a pipe under a definition of the non-linear behavior of the soil. It will also be necessary to study the seismic response of the pipes using models with several layers of soil in both the vertical and horizontal directions. Finally, the effect of different diameters on the tension of the rings will have to be investigated.

Acknowledgements

We acknowledge IPN-SIP research projects 20201923 and 20211972.

Conflicts of Interest

The authors declare no conflict of interest.

References

[1] Casanova-del-Angel, F. and Córdova-Castillo, A. (2018) Metallography of an Underground Oil Pipeline. *Open Journal of Metal*, **8**, 35-54. https://doi.org/10.4236/ojmetal.2018.83003

[2] Leyva Trujillo, M. and Salazar Arguello, S.I. (2017) Emisiones, fugas y derrames en el transporte de hidrocarburos por ductos. Tesis conjunta para obtener el título de ingeniero petrolero. Ciudad Universitaria, Ciudad de México..

[3] Mahmood, D.N. and Abdulrazzaq, O.A. (2020) Stress Analysis of Buried Pipeline Using Finite Element Method. *Journal of University of Babylon for Engineering Sciences*, **28**, 846-850.

[4] Lee, H. (2010) Finite Element Analysis of a Buried Pipeline. School of Mechanical, Aerospace and Civil Engineering. Master's Thesis, University of Manchester, Manchester.

[5] Hernández, A.H. (1991) Análisis de falla por fractura en tuberías de conducción de petróleo. *Ingeniería e Investigación*, 25-36. https://doi.org/10.15446/ing.investig.n23.20677

[6] Nair, P. and Naik, S. (2017) Stress Analysis of Buried Pipelines. *International Research Journal of Engineering and Technology*, **4**, 11-24.

[7] Sharp, K.D., Anderson Loren, R., Moser, A.P. and Bishop Ronald, R. (1985) Finite Element Analysis Applied to the Response of Buried FRP Pipe under Various Installation Conditions. *Transportation Research Record*, **1008**, 497-508.

[8] Griffith, A.A. (1921) The Phenomena of Rupture and Flow in Solids. Philosophical Transactions of the Royal Society of London Series A, Containing Papers of a Mathematical or Physical Character, 221, 163-198.

https://doi.org/10.1098/rsta.1921.0006

[9] Irwin, G.R. (1948) Fracture Dynamics, Fracturing of Metals. American Society for Metals, Cleveland, 147-166.

[10] Orowan, E. (1949) Fracture Strength of Solids. *Reports of Progress in Physics*, **12**, 185. https://doi.org/10.1088/0034-4885/12/1/309

[11] (2001) ASME B31.8, Gas Transmission and Distribution Piping Systems.

[12] (2009) NRF-030-PEMEX-2009, Diseño, construcción, inspección y mantenimiento de ductos terrestres para transporte y recolección de hidrocarburos.

[13] American Petroleum Institute (2004) API 5L, Specification for line pipe. Forty-fourth Edition.

[14] (2001) ASCE, Guideline for the Design of Buried Steel Pipe.

[15] Crespo Villalaz, C. (2004) Mecánica de suelos y cimentaciones. 5ª edición, Editorial Limusa.